Turk J Chem
33 (2009) , 825 – 841.

doi:10.3906/kim-0809-33

Partial regeneration of Ni-based catalysts for hydrogen production via methane cracking part II: modeling and optimization

Reyyan KOÇ[1,*], Erdoğan ALPER[1], Eric CROISET[2] and Ali ELKAMEL[2]
[1] *Chemical Engineering Department, Hacettepe University, Beytepe, Ankara-TURKEY*
e-mail: rkoc@hacettepe.edu.tr, ealper@hacettepe.edu.tr
[2] *Chemical Engineering Department, University of Waterloo, Waterloo, Ontario-CANADA*
e-mail: ecroiset@uwaterloo.ca, aelkamel@uwaterloo.ca

Received 17.09.2008

High purity, carbon monoxide-free hydrogen and filamentous carbon can be produced by thermo-catalytic cracking of methane. Carbon filaments continue to grow until the catalyst deactivates because of carbon encapsulation. Regeneration of catalyst is important to maintain a continuous process. Our work on optimization of the partial regeneration method showed that activity of the catalyst can be sustained for longer times by gasifying not all but some extent of the deposited carbon. In the previous work, a kinetic model was developed to be able to understand the reaction mechanism of deactivation of fresh catalyst at the molecular level. The objective of this study was to develop a well-fitted kinetic model for deactivation of regenerated catalyst.

A kinetic model that consists of surface reactions, filament formation, and deactivation was developed for the regenerated catalyst. It is assumed that reaction parameters at the molecular level do not change when the burn off degree is at a moderate extent but these parameters changed drastically when burn off degree is vastly increased or decreased.

Rate constant for the encapsulation reaction is adjusted for the simulation results to be representative of the experimental results (typically specific weight of carbon (g C/g Ni) vs. time on stream). The system of differential algebraic equations consists of the steady-state equations for all surface intermediates, an algebraic equation of dissolution/segregation, diffusion equation, and the site balance equation. The system has been solved without assuming any rate-determining step or most abundant surface intermediates.

*Corresponding author

Parameter estimation procedures were repeated for the deactivation cycles of regenerated 5 wt% Ni/γ-Al_2O_3 catalyst. The basic idea that underlies the model is that every carbon atom will diffuse through the nickel particle and participate in the formation of carbon filaments until the catalyst deactivates. Specific weight of carbon is calculated using the rate of carbon diffusion.

Key Words: Thermo catalytic cracking of methane, hydrogen, filamentous carbon, partial regeneration, Ni/γ-Al_2O_3 catalyst, kinetic modeling, estimation of rate constant.

Introduction

It is possible to produce pure hydrogen by thermo-catalytic cracking of methane at moderate temperatures. Methane decomposition on nickel based catalysts is a technologically simple one-step process without energy and material intensive gas separation stages and shows the potential to be a CO_2-free hydrogen production process. This feature of catalytic cracking of methane makes the process suitable especially for PEM fuel cell applications.[1–3] In addition, pure carbon, the second product, instead of carbon monoxide and carbon dioxide, has various applications such as catalyst supports, reinforcement material, selective adsorption agents, and in energy storage devices.[4]

Whilst miscellaneous catalysts were used for methane cracking, nickel supported on gamma alumina was selected as the catalyst in this work. As the methane decomposes to carbon and hydrogen, carbon filaments continue to grow as hollow channels on the catalyst. At the end catalyst deactivates due to encapsulation. The reason for deactivation is carbon encapsulation, which hinders the interaction between active metal particles and methane, not the detachment of the metal particle.[5] It has been shown that the catalyst life mainly depends on the morphology of the deposited carbon, which grows either as filamentous carbon or encapsulated carbon. Formation of filaments extends the life time of the catalyst.[6] Deactivation of the catalyst is still a problem for the sustainability of the process and to address this concern we regenerated the catalyst by partial oxidation of accumulated carbon.

The growth of carbon filaments is a result of the following processes: decomposition of the hydrocarbon at the gas–metal interface followed by dissolution of carbon into the metal and diffusion through the particle. The carbon then precipitates at the metal–support interface, detaches the metal particle from the support and forms a filament with an exposed metal particle at its tip. The rate-determining step of this process is thought to be the diffusion of carbon through the metal particle. This mode of carbon accumulation allows the catalyst to maintain its activity for an extended period of time without deactivation;[2,4] However, if methane cracking is to be utilized for the production of hydrogen in a continuous process catalyst regeneration has to be improved. Such regeneration is still being investigated in order to render the process continuous and economically viable. That is why the present study focuses on regeneration of the nickel supported on alumina. Our previous work on 5-wt% Ni/γ-Al_2O_3 indicated that after complete gasification of the carbon, the catalyst has lost nearly all its activity toward methane cracking.[2] Instead of complete gasification, partial gasification of the deposited carbon is a strategy that we propose to maintain significant activity of the catalyst. This technique, also known as partial regeneration, is a promising strategy to overcome the challenge of catalyst deactivation in the catalytic decomposition of methane. This study extends our previous work and attempts to investigate the effects of percentage of nickel, application of reduction, reaction temperature, and amount of gasified carbon and particle

arrangement on catalyst activity. The textural and morphological properties of the combination of carbon filaments and Ni/γ-Al_2O_3 catalyst have been investigated by SEM/EDS and BET analysis. A kinetic model that consists of surface reactions, formation of carbon filaments, and catalyst deactivation is also presented.

In the kinetic modeling, the reaction mechanisms are analyzed at the molecular level to improve the activity of the catalyst. The kinetic expressions are traditionally derived from the Langmuir-Hinshelwood approach. In this approach, a rate-determining step (RDS) is assumed and the possible effect of coke formation on the RDS has usually been ignored.[7] Reaction conditions can be effective on the RDS or multiple RDSs can exist.[8] Unlike this traditional approach, a more fundamental kinetic model is presented for describing the effects in catalyst deactivation. In the previous work, a kinetic model was developed based on the knowledge of elementary reaction steps and their energetic without assuming any RDS or abundant surface species.[2] Experimental data obtained from deactivation of fresh catalyst are used for parameter estimation. Weight gain resulting from carbon deposition and weight loss resulting from partial gasification with air were recorded by a thermo gravimetric analyzer and the data were used for calculating the activity of the catalyst in the experimental part of this work. Different catalytic activities were obtained for different nickel percentages, amounts of gasified carbon, and reaction temperatures. The kinetic parameters that are closely related to the yield of methane decomposition will change with changing catalyst specifications and regeneration conditions. The kinetic modeling for deactivation cycles of regenerated catalyst may ensure a better understanding for deactivation that may be useful to achieve higher methane conversion and longer catalyst life times.

Experimental

The catalysts used for thermo-catalytic cracking of methane were 5, 10, and 15 wt% Ni/γ-Al_2O_3 (30-40 mesh) prepared by incipient wetness impregnation. Only the experimental results of 5 wt% Ni/γ-Al_2O_3 are used in this study. Calcination, reduction, methane cracking reaction, and partial regeneration were performed in situ in the thermo gravimetric analyzer (Cahn TG 151 manufactured by Thermo Cahn). Detailed procedures for catalyst preparation, pretreatment, activity measurement, and partial regeneration method are elucidated in the previous experimental work.[9]

Kinetic modeling of carbon deposition by thermo-catalytic cracking of methane on nickel based catalysts

The kinetic model consists of 3 main parts: surface reactions, carbon filament formation, and catalyst deactivation.

Surface reactions

The chemisorption of methane is dissociative and that the nascent product of the dissociative chemisorption is an adsorbed methyl group that gradually dehydrogenates on the surface at higher temperatures. The model includes the following elementary reaction steps on the nickel surface:[10]

$$CH_4 + 2S \Leftrightarrow CH_3.S + H.S \quad (1)$$

$$CH_3.S + S \Leftrightarrow CH_2.S + H.S \tag{2}$$

$$CH_2.S + S \Leftrightarrow CH.S + H.S \tag{3}$$

$$CH.S + S \Leftrightarrow C.S + H.S \tag{4}$$

$$2H.S \Leftrightarrow H_2 + 2S \tag{5}$$

The Langmuir-Hinsellwood approach is adopted for the quantitative formulation of the kinetics of thermo-catalytic cracking of methane over Ni based catalyst. CH_4, CH_3, CH_2, CH, C, H, and H_2 are the chemical species take part in the interaction and S is the active catalyst site.[11–13]

The filament formation

The surface reactions produce adsorbed carbon atoms. Other types of surface carbon that may encapsulate the surface can also be formed. The isolated surface carbon atoms that are important in the filament formation dissolve into the nickel particle at the gas side, and diffuse to the rear, at the support side and precipitate at the rear of the nickel particle and form the filament.[14] Carbon formation by cracking has been studied extensively and more information can be obtained from the literature.[15–23]

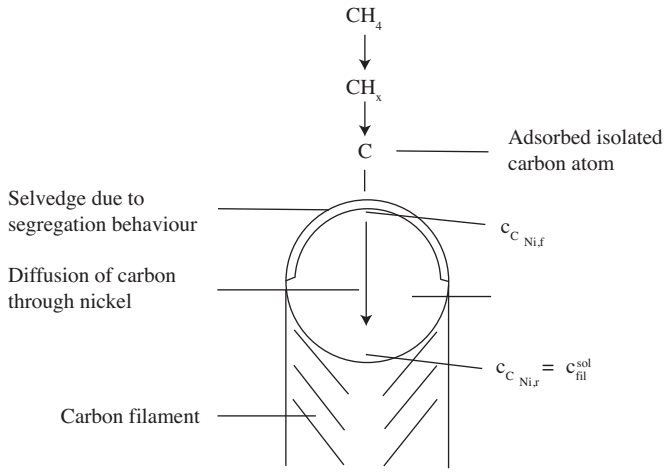

Figure 1. Detailed mechanism of the filamentous carbon formation by methane cracking.[14]

The detailed mechanism for the formation of filamentous carbon is schematically represented for methane cracking in Figure 1. The model includes the dissolution/segregation and diffusion and precipitation steps as follows.

Dissolution/Segregation:

$$C.S \Leftrightarrow C_{Ni,F} + S \tag{6}$$

At the front of the nickel particle, a selvedge with high concentration is created because of the segregation behavior of carbon in nickel; the surface is enriched with carbon, and the carbon concentration decreases from the surface concentration to the bulk concentration of interstitially dissolved carbon over a number of atomic

layers. The relation between the surface coverage of carbon and the bulk concentration of interstitially dissolved carbon in nickel, just below the selvedge, can be described by a segregation isotherm.

The complex of carbon atom with the active surface, "C.S", was described as the adsorbed atomic carbon.[14] The following equation (E.1) can be applied to estimate the concentration of carbon in the segregation layer. A Langmuir equation for the segregation was selected to estimate the concentration of carbon in the segregation layer.[10]

$$\frac{\theta_{C.S}}{1-\theta_{C.S}} = \frac{x_F}{1-x_F}\exp\left(-\frac{\Delta G_{seg}}{RT}\right) \tag{E.1}$$

where $\theta_{C.S}$ is the surface coverage of carbon, with ΔG_{seg} = –45,217 – 14.24 T (J/mol).[14]

Diffusion of Carbon through Nickel:

$$C_{Ni,F} \Rightarrow C_{Ni,R} \tag{7}$$

The different chemical potentials of different carbon materials result in different solubility at the front and the rear of the nickel crystallite. It creates a driving force for the diffusion of carbon through the nickel.[10] The rate of carbon diffusion through the nickel can be written in Fick's law:

$$r_7 = \frac{D_{C_{Ni}}}{l}.(x_{C_{Ni,F}} - x_{C_{Ni,R}}).A_{Ni} \tag{E.2}$$

where r_7 is the rate of carbon diffusion through nickel (mol C. g cat^{-1}. h^{-1}); the average path length which is assumed as the 2/3 of nickel diameter; $D_{C_{Ni}}$ Diffusivity of carbon in nickel; $x_{C_{Ni,F}}$, concentration of carbon dissolved in nickel at the front of Ni (mol C/m^3); $x_{C_{Ni,R}}$,concentration of carbon dissolved in nickel at the rear of Ni (mol C/m^3); A_{Ni}, specific surface area of nickel particle

Precipitation/Dissolution:

$$C_{Ni,R} \Leftrightarrow C_f \tag{8}$$

A carbon filament precipitates at the support side of the nickel particle. It is assumed during the modeling that precipitation/dissolution reaction is too fast. That is why every atom that reaches the rear end of the nickel particle immediately combines with the structure of the filaments.[14]

Catalyst deactivation

As the methane cracking reaction goes on, while a larger part of the deposited carbon diffuses into the nickel to form the filaments, a smaller amount of deposited carbon encapsulates the active surfaces. At the end all of the active sites will be covered by the encapsulating carbon and the interface between the gas phase and active nickel sites will be blocked. Therefore, it is assumed that the changes in the surface coverage of encapsulating carbon are the main cause of deactivation.

Encapsulating carbon formation:

$$nC.S \Rightarrow nC_p \tag{9}$$

The atomic carbon on the surface is a common intermediate in the filamentous and encapsulating carbon formation.[16–18] The reaction between the adsorbed carbon at the surface is assumed to be irreversible and the sole pathway for encapsulating carbon formation. The rate expression can be written for this equation as

$$r_9 = k_9 \theta_{C.S}^n$$

where k_9 [molecule/(site.min)] is the encapsulation rate constant and n is related to the ensemble size of the encapsulated carbon formation. According to Chen et al.,[10] an ensemble size of 6 for encapsulated carbon formation (n = 3) gave the best fit of the experimental results.

The encapsulating carbon deactivates the catalysts by decreasing the total number of active sites. This is described by a site conservation balance equation (E.3) as follows:[2]

$$\theta_t = \theta_{CH_3.S} + \theta_{CH_2.S} + \theta_{CH.S} + \theta_{C.S} + \theta_{H.S} + \theta_v + \theta_p \tag{E.3}$$

where θ_t is the total active site concentration and equals one. θ_p is the fractional surface coverage of the encapsulated carbon.

More details about the model, the rate equations and their derivations, and initial conditions are given in the appendix and the solution approach is highlighted in the next section. The stiff ordinary differential equation solver (Ode23s) in MATLAB was employed to solve the model. The unknown parameters in the model were estimated through a parameter estimation procedure using the experimental data points collected whereby the set of best parameters that minimize the sum of square errors between the model and data was considered. More details are given in the next section on the parameters that were estimated using this parameter estimation approach and those that were obtained from the literature.

Application of kinetic modeling

In the kinetic model, the rate constants of surface reaction, physical properties of the nickel particle, Langmuir equation for the segregation, and exponent "n" for the encapsulating carbon step are taken from the data given by Chen et al.[10] and Snoeck et al.[14] whereas rate constant for the encapsulation reaction is adjusted for the simulation results to be representative of the experimental results (typically specific weight of carbon, g C/g Ni, vs. time on stream). The system of differential algebraic equations consists of the steady-state equations for all surface intermediates, an algebraic equation of dissolution/segregation, diffusion equation, and the site balance equation. The system has been solved without assuming any rate-determining step or most abundant surface intermediates. One solid solute concentration (concentration of carbon in nickel at the front of the particle, x_F) and 7 surface species have been solved from 6 nonlinear differential equations and 2 algebraic equations.

Parameter estimation procedures were repeated for the deactivation cycles of regenerated 5 wt% Ni/γ-Al_2O_3 catalyst (see Table). The basic idea the underlies the model is that every carbon atom will diffuse through the nickel particle and participate in the formation of carbon filaments until the catalyst deactivates. Specific weight of carbon is calculated using the rate of carbon diffusion.

Rate constants of deactivation cycles of 5 wt% Ni/γ-Al_2O_3 catalyst in Figures 3 to 6 are 5.3, 6.3, 14.85, and 0.84 min^{-1}, respectively. The model matches reasonably well the experimental data. For the first 3 figures, the percentage of gasified carbon is 8.6 wt %, and encapsulation reaction in the second and fourth deactivation

is faster than the first one. However, when the percentage of gasified carbon was increased to 91.3 wt %, the rate of encapsulation reaction in the fourth deactivation cycle dropped drastically to 0.84 min^{-1}.

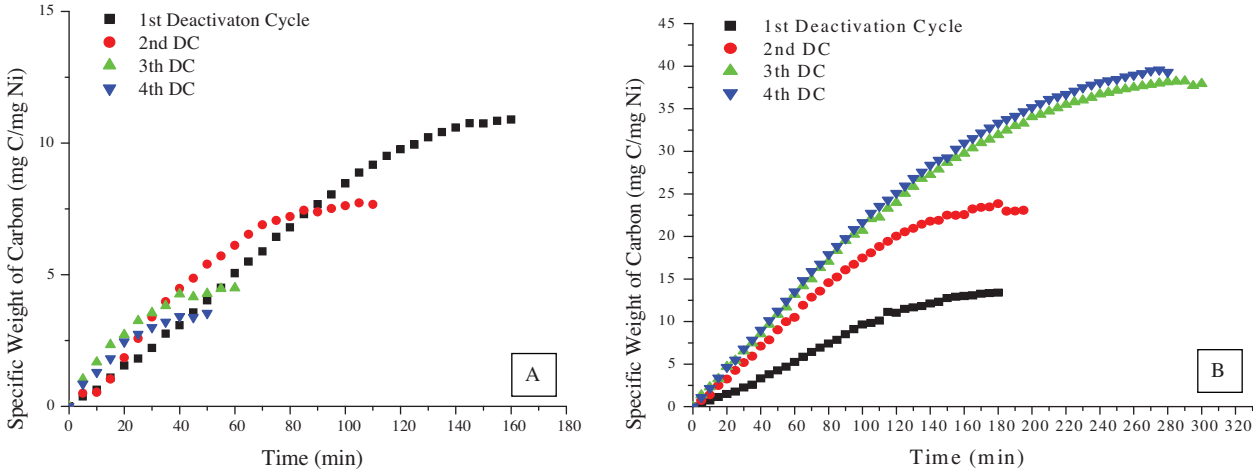

Figure 2. Experimental results: Specific weight of carbon over time for separate deactivation cycles of each continues deactivation-regeneration run[9]. A) 5 wt % $Ni/\gamma\text{-}Al_2O_3$, T = 500 °C, BOD = 8.63; B) 5 wt % $Ni/\gamma\text{-}Al_2O_3$, T = 500 °C, BOD = 91.27.

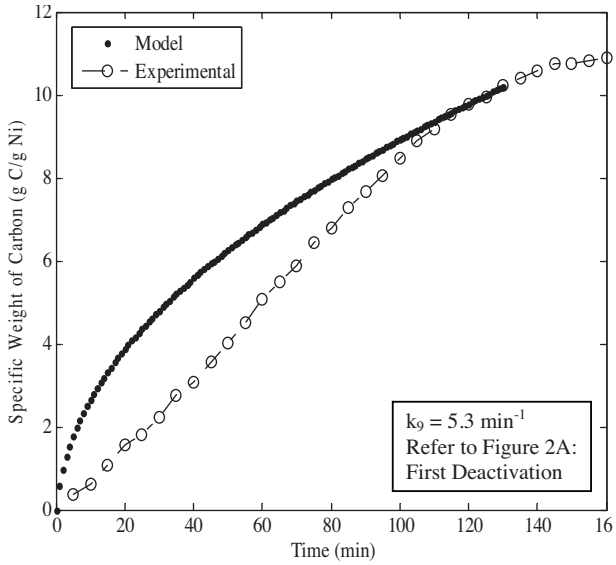

Figure 3. Calculated (•) and experimental (○) specific weight of carbon over time for the first deactivation cycle of 5 wt% $Ni/\gamma\text{-}Al_2O_3$ catalyst with BOD = 8.63.

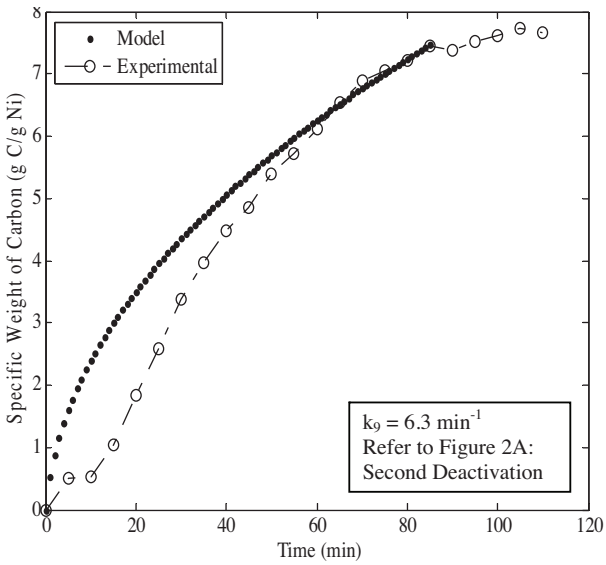

Figure 4. Calculated (•) and experimental (○) specific weight of carbon over time for the second deactivation cycle of 5 wt% $Ni/\gamma\text{-}Al_2O_3$ catalyst with BOD = 8.63.

Although the model provides a close estimation for the determination of weight gain during the thermo-catalytic cracking of methane, it fails at the initial stage of carbon deposition and gives higher rates of carbon deposition than the actual one.

Table. Sample properties and deactivation and regeneration specifications.[9]

Sample	Total Specific Weight Gain (mg C/mg Ni)	Average of % Burn off
5-wt % Ni, T= 500 °C	26.59	8.63
5-wt % Ni, T= 500 °C	113.97	91.27

T: Reaction Temperature

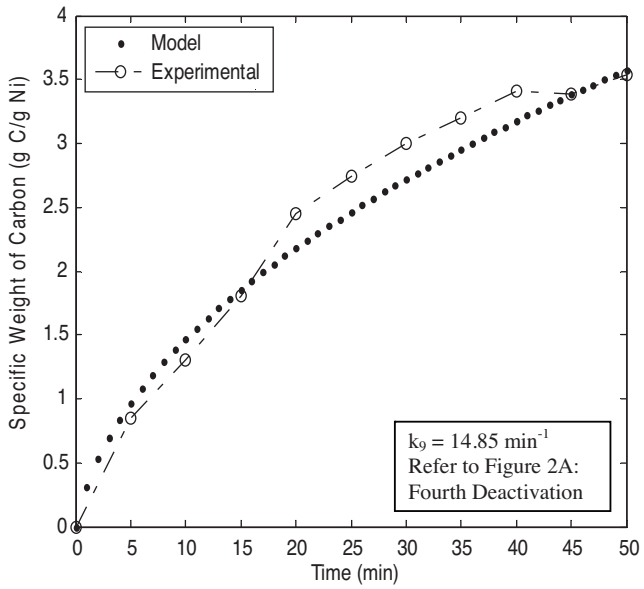

Figure 5. Calculated (•) and experimental (∘) specific weight of carbon over time for the fourth deactivation cycle of 5 wt% $Ni/\gamma\text{-}Al_2O_3$ catalyst with BOD = 8.63.

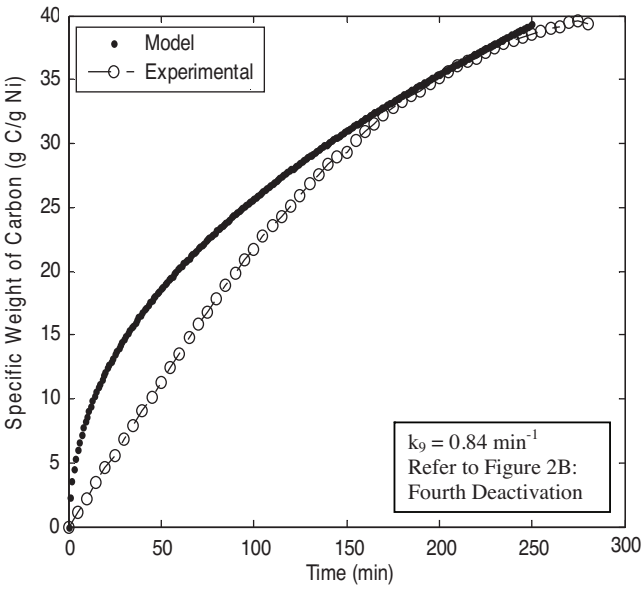

Figure 6. Calculated (•) and experimental (∘) specific weight of carbon over time for the fourth deactivation cycle of 5 wt% $Ni/\gamma\text{-}Al_2O_3$ catalyst with BOD = 91.27.

Conclusions

A kinetic model that consists of 3 main parts, namely surface reactions, carbon filament formation, and catalyst deactivation, had been developed. Some agreement on the general trends between the model and experimental results was obtained. The encapsulation reaction was assumed as the only reason for deactivation when the amount of gasified carbon was low. The unknown rate constant of the encapsulation reaction was estimated for the regenerated catalyst. The rate constant of the encapsulation reaction increased while causing a decrease in the activity of the $Ni/\gamma\text{-}Al_2O_3$ catalysts after regeneration when the amount of gasified carbon was low; in contrast it decreased when the amount of gasified carbon was high and so the activity of the catalyst increased.

The approximations that are made for the kinetic model may affect the efficiency of the model. Firstly, the carbon concentration at the rear end of the filament was assumed as zero because the rate of the reaction in which carbon atoms combines into filaments was assumed to be too fast. Additionally, x_F (concentration

of carbon in the bulk of the nickel at the front side of Ni particle) is calculated from the Langmuir equation, which is also based on approximations. The distribution of Ni particle size and reconstruction in the particle shape during the carbon formation are not considered in the model; uniform distribution of nickel particles on the catalyst and equal size of each particle are presumed.

Nomenclature and Abbreviations

A_{Ni}	Specific surface area of nickel particle [m^2 / g cat]
$C_{C_{Ni,F}}$	Concentration of carbon dissolved in nickel at the front of the particle [mol C/m^3]
$C_{C_{Ni,R}}$	Concentration of carbon dissolved in nickel at the rear of the particle [mol C/m^3]
d_{Ni}	Diameter of the nickel particle [nm]
$D_{C_{Ni}}$	Diffusivity of carbon in nickel [m^2 / h]
ΔG_{seg}	Change of energy for segregation of carbon [J/mol]
(g)	Gaseous phase
k_1	forward rate constant of the reaction step (1) [molecule / (site .min .atm)]
k_2	reverse rate constant of the reaction step (1) [molecule / (site .min)]
k_3	forward rate constant of the reaction step (2) [molecule / (site .min)]
k_4	reverse rate constant of the reaction step (2) [molecule / (site .min)]
k_5	forward rate constant of the reaction step (3) [molecule / (site .min)]
k_6	reverse rate constant of the reaction step (3) [molecule / (site .min)]
k_7	forward rate constant of the reaction step (4) [molecule / (site .min)]
k_8	reverse rate constant of the reaction step (4) [molecule / (site .min)]
k_9	forward rate constant of the reaction step (5) [molecule / (site .min)]
k_{10}	reverse rate constant of the reaction step (5) [molecule / (site .min .atm)]
k_{11}	encapsulation rate constant of the reaction step (9) [molecule / (site .min)]
l	Diffusion path length [m]
P_{CH_4}	Partial pressure of methane [atm]
P_{H_2}	Partial pressure of hydrogen [atm]
r	rate of carbon formation [g C/ (g Ni.min)]
r_1	rate of reaction for the step (1) [molecule / (site .min)]
r_2	rate of reaction for the step (2) [molecule / (site .min)]
r_3	rate of reaction for the step (3) [molecule / (site .min)]
r_4	rate of reaction for the step (4) [molecule / (site .min)]
r_5	rate of reaction for the step (5) [molecule / (site .min)]
r_6	rate of encapsulation of adsorbed carbon [molecule / (site .min)]
R	Universal gas constant [J/ (mol.K)]
S	Active site of the metal
(S)	Solid phase
T	Temperature
x_F	Concentration of carbon at the front of the bulk of the nickel particle [gram C per gram Ni]

x_R	Concentration of carbon at the rear of the bulk of the nickel particle [gram C per gram Ni]
x_{sat}	Saturation concentration of filamentous carbon in Ni [mol C/m^3]

Greek

$\theta_{i.s}$	fractional surface concentration of sites occupied by species i (no unit)
	$i =$ CH_3, CH_2, CH, C and H
θ_t	total active sites
θ_v	fractional coverage of vacant site
ρ_{Ni}	density of nickel [g/m^3]
η	number of surface metal atoms

Subscripts

avr	average
BET	Brunauer, Emmett, and Teller
C	carbon
C $_{Diff}$	carbon diffusion
cat	catalyst
Ni	nickel
r	reverse
(s)	adsorbed on surface
S	surface
seg	segregation
SEM	Scanning Electron Microscopy
sol	solution
t	total
Trans	translational
V	vacant site
W	the final carbon phase, whisker

Acknowledgements

One of the authors, Reyyan Koç, would like to thank the Natural Science and Engineering Research Council of Canada for the financial support.

References

1. Rahman, M.; Croiset, E.; Elkamel, A., *Topics in Catalysis*, **2006**, *37*, 137-145.
2. Hazra, M.; Croiset, E.; Elkamel, A., *Proceedings International Hydrogen Energy Congress and Exhibition IHEC*, 13-15 July **2005**, Istanbul, Turkey,
3. Muradov, N.Z., *Energy & Fuels*, **1998**, *12*, 41-48.
4. Choudhary, T.V.; Aksoylu, E.; Goodman, D.W., *Catalysis Reviews*, **2003**, *45*, 151–203.
5. Trimm, D. L.,*Catalysis Today*, **1999**, *49*, 3-10.
6. Echegoyen, Y.; Suelves, I.; Lazaro, M.J.; Moliner, R.; Palacios, J.M. *Journal of Power Sources*, **2007**, *169*, 150-157.
7. Minot, C.; Van Hove, M. A.; Somorjai, G. A., *Surf. Sci.,* **1982**, *127*, 441.
8. Dumesic, J.A.; Rudd, D.F.; Aparicio, L.M.; Rekoske, J.E.; Trevino, A.A., *The Microkinetics of Heterogeneous Catalysis*, **1993**, American Chemical Society, Washington, DC.
9. Koç, R.; Alper, E.; Croiset, E.; Elkamel, A. *Turk J. Chem*, **2008**, *32*, 157-168
10. Chen, D.; Lodeng, R.; Anundskas, A.; Olsvik, O.; Holmen, A., *Chem. Eng. Science,* **2001**, *56*, 1371-1379.
11. Ceyer, S.T., *Ann. Rev. Phy. Chem.*, **1988**, *39*, 479-510.
12. Solymosi, F.; Erdohelyi, A.; Cserenyi, J.; Felvegi, A. *J. Catal.,* **1994**, *147*, 272-278.
13. Bianchini, E.C.; Lund, C.R.F., *J. Catal.* , **1989**, *117,* 455-466.
14. Snoeck, J. W.; Froment, G. F.; Fowlesz, M., *J. of Catal.*, **1997a**, *169*, 240-249.
15. Shaikhutdinov, S. K.; Avdeeva, L. B.; Goncharova, O. V.; Novgorodov B. N., *Appl. Catal. A,* **1995**, *126,* 125-139.
16. Kuvshinov, G.G.; Mogilnykh, Y.I.; Kuvshinov, D.G.; Zaikovskii, V.I.; Avdeeva, L.B., *Carbon,* **1998**, *36*, 87-97.
17. Shaikhutdinov, S.K.; Avdeeva, L.B.; Novgorodov, B.N.; Zaikovskii, V.I.; Kochubey, D.I., *Catal. Lett.*, **1997**, *47*, 35-42.
18. Takenaka, S.; Ogihara, H.; Otsuka, K., *J. Catal.*, **2002**, *208*, 54-63.
19. Yongdan, L.; Chen, J.; Chang, L.; Qin Y., *J. Catal.*, **1998***, 178*, 76-83.
20. Fogler, H.S., *Elements of Chemical Reaction Engineering*, Prentice Hall Int., New Jersey, 1999.
21. Isett, L.C. and Blakely J.M., *Surf. Sci.*, **1976**, *58*, 397-414.
22. Penchev, V.; Neynska, Y.; Kanazirev, V., *Preparation of Catalysts II*, Elsevier, Amsterdam, **1979**, 497.
23. Baker, R.T.K.; Barber, M.A.; Waite, R.J.; Harris, P.S.; Feates, F.S., *J. Catal.*, **1972**, *26*, 51-62.

APPENDIX: Derivation of rate equations

$\mathrm{P}\ (1) = \mathrm{P}_{CH4}\,,\ \mathrm{P}\ (2) = \mathrm{P}_{H2}$

$\theta_{CH_3.S} = x_1, \theta_{CH_2.S} = x_2, \theta_{CH.S} = x_3, \theta_{C.S} = x_4, \theta_{H.S} = x_5, \theta_{encapsulated} = x_6, \theta_{vacant} = x_7,$

$x_F (C_{Ni,F} = x_F * 7.42e5)$

where

C_v is the number of vacant sites per unit mass of catalyst divided by Avogadro's number. (gmol/gcat)
$C_{i.S}$ is the surface concentration of sites occupied by species i. (gmol/gcat)
$\theta_{i.S} = \frac{C_{i.S}}{C_{total}}$ (Number of sites occupied by species i / Number of active sites)

1. $CH_4 + 2S \xrightarrow{k_1'} CH_3.S + H.S$

$CH_3.S + H.S \xrightarrow{k_2'} CH_4 + 2S \quad -r_{CH_4} = r_{CH_3.S}$

$$\left[\frac{dC_{CH_3.S}}{dt}\right]_{R1} = k_1' C_\nu^2 P_{CH_4} - k_2' C_{CH_3.S} C_{H.S}$$

$$\left[\frac{d(\theta_{CH_3.S} C_{tot})}{dt}\right]_{R1} = k_1' C_\nu^2 P_{CH_4} - k_2' C_{CH_3.S} C_{H.S}$$

$$C_{tot}\left[\frac{d\theta_{CH_3.S}}{dt}\right]_{R1} = k_1' C_\nu^2 P_{CH_4} - k_2' C_{CH_3.S} C_{H.S}$$

$$\left[\frac{d\theta_{CH_3.S}}{dt}\right]_{R1} = \frac{1}{C_{tot}} k_1' C_\nu C_\nu P_{CH_4} - \frac{1}{C_{tot}} k_2' C_{CH_3.S} C_{H.S} \quad \text{Multiply by } \frac{C_{tot}}{C_{tot}}$$

$$\left[\frac{d\theta_{CH_3.S}}{dt}\right]_{R1} = \underbrace{C_{tot} k_1'}_{k_1} \frac{C_\nu}{C_{tot}} \frac{C_\nu}{C_{tot}} P_{CH_4} - \underbrace{C_{tot} k_2'}_{k_2} \frac{C_{CH_3.S}}{C_{tot}} \frac{C_{H.S}}{C_{tot}}$$

$$\left[\frac{d\theta_{CH_3.S}}{dt}\right]_{R1} = k_1 \theta_v^2 P_{CH_4} - k_2 \theta_{CH_3.S} \theta_{H.S}$$

$$r_1 = k_1 P_{CH_4} \theta_v^2 - k_2 \theta_{CH_3.S} \theta_{H.S}$$

2. $CH_3.S + S \xrightarrow{k_3'} CH_2.S + H.S$

$CH_2.S + H.S \xrightarrow{k_4'} CH_3.S + S \quad -r_{CH_3.S} = r_{CH_2.S}$

$$\left[\frac{dC_{CH_2.S}}{dt}\right]_{R2} = k_3' C_{CH_3.S} C_\nu - k_4' C_{CH_2.S} C_{H.S}$$

$$\left[\frac{d(\theta_{CH_2.S}C_{tot})}{dt}\right]_{R2} = k_3' C_{CH_3.S} C_\nu - k_4' C_{CH_2.S} C_{H.S}$$

$$\left[\frac{d\theta_{CH_2.S}}{dt}\right]_{R2} = \frac{1}{C_{tot}} k_3' C_{CH_3.S} C_\nu - \frac{1}{C_{tot}} k_4' C_{CH_2.S} C_{H.S}$$

$$\left[\frac{d\theta_{CH_2.S}}{dt}\right]_{R2} = \underbrace{C_{tot} k_3'}_{k_3} \frac{C_{CH_3.S}}{C_{tot}} \frac{C_\nu}{C_{tot}} - \underbrace{C_{tot} k_4'}_{k_4} \frac{C_{CH_2.S}}{C_{tot}} \frac{C_{H.S}}{C_{tot}}$$

$$\left[\frac{d\theta_{CH_2.S}}{dt}\right]_{R2} = k_3 \theta_{CH_3.S} \theta_v - k_4 \theta_{CH_2.S} \theta_{H.S}$$

$$r_2 = k_3 \theta_{CH_3.S} \theta_v - k_4 \theta_{CH_2.S} \theta_{H.S}$$

3. $CH_2.S + S \xrightarrow{k_5'} CH.S + H.S$

   $CH.S + H.S \xrightarrow{k_6'} CH_2.S + S \quad -r_{CH_2.S} = r_{CH.S}$

$$\left[\frac{dC_{CH.S}}{dt}\right]_{R3} = k_5' C_{CH_2.S} C_\nu - k_6' C_{CH.S} C_{H.S}$$

$$\left[\frac{d(\theta_{CH.S}C_{tot})}{dt}\right]_{R3} = k_5' C_{CH_2.S} C_\nu - k_6' C_{CH.S} C_{H.S}$$

$$\left[\frac{d\theta_{CH.S}}{dt}\right]_{R3} = \frac{1}{C_{tot}} k_5' C_{CH_2.S} C_\nu - \frac{1}{C_{tot}} k_6' C_{CH.S} C_{H.S}$$

$$\left[\frac{d\theta_{CH.S}}{dt}\right]_{R3} = \underbrace{C_{tot} k_5'}_{k_5} \frac{C_{CH_2.S}}{C_{tot}} \frac{C_\nu}{C_{tot}} - \underbrace{C_{tot} k_6'}_{k_6} \frac{C_{CH.S}}{C_{tot}} \frac{C_{H.S}}{C_{tot}}$$

$$\left[\frac{d\theta_{CH.S}}{dt}\right]_{R3} = k_5 \theta_{CH_2.S} \theta_v - k_6 \theta_{CH.S} \theta_{H.S}$$

$$r_3 = k_5 \theta_{CH_2.S} \theta_v - k_6 \theta_{CH.S} \theta_{H.S}$$

4. $CH.S + S \xrightarrow{k_7'} C.S + H.S$

   $C.S + H.S \xrightarrow{k_8'} CH.S + S \quad -r_{CH.S} = r_{C.S}$

$$\left[\frac{dC_{C.S}}{dt}\right]_{R4} = k_7' C_{CH.S} C_\nu - k_8' C_{C.S} C_{H.S}$$

$$\left[\frac{d(\theta_{C.S}C_{tot})}{dt}\right]_{R4} = k'_7 C_{CH.S} C_\nu - k'_8 C_{C.S} C_{H.S}$$

$$\left[\frac{d\theta_{C.S}}{dt}\right]_{R4} = \frac{1}{C_{tot}} k'_7 C_{CH.S} C_\nu - \frac{1}{C_{tot}} k'_8 C_{C.S} C_{H.S}$$

$$\left[\frac{d\theta_{C.S}}{dt}\right]_{R4} = \underbrace{C_{tot} k'_7}_{k_7} \frac{C_{CH.S}}{C_{tot}} \frac{C_\nu}{C_{tot}} - \underbrace{C_{tot} k'_8}_{k_8} \frac{C_{C.S}}{C_{tot}} \frac{C_{H.S}}{C_{tot}}$$

$$\left[\frac{d\theta_{C.S}}{dt}\right]_{R4} = k_7 \theta_{CH.S} \theta_v - k_8 \theta_{C.S} \theta_{H.S}$$

$$r_4 = k_7 \theta_{CH.S} \theta_v - k_8 \theta_{C.S} \theta_{H.S}$$

5. $2H.S \xrightarrow{k'_9} H_2 + 2S$

   $H_2 + 2S \xrightarrow{k'_{10}} 2H.S \quad \frac{-r_{H.S}}{2} = \frac{r_{H_2}}{1}$

$$\left[-\frac{dC_{H.S}}{dt}\right]_{R5} = 2(k'_9 C^2_{H.S} - k'_{10} P_{H_2} C^2_v)$$

$$\left[-\frac{d(\theta_{H.S}C_{tot})}{dt}\right]_{R5} = 2(k'_9 C^2_{H.S} - k'_{10} P_{H_2} C^2_v)$$

$$\left[-\frac{d\theta_{H.S}}{dt}\right]_{R5} = 2(\frac{1}{C_{tot}} k'_9 C^2_{H.S} - \frac{1}{C_{tot}} k'_{10} P_{H_2} C^2_v)$$

$$\left[-\frac{d\theta_{H.S}}{dt}\right]_{R5} = 2(\underbrace{C_{tot} k'_9}_{k_9} \frac{C_{H.S}}{C_{tot}} \frac{C_{H.S}}{C_{tot}} - \underbrace{C_{tot} k'_{10}}_{k_{10}} P_{H_2} \frac{C_v}{C_{tot}} \frac{C_v}{C_{tot}})$$

$$\left[-\frac{d\theta_{H.S}}{dt}\right]_{R5} = 2(k_9 \theta^2_{H.S} - k_{10} \theta^2_v P_{H_2})$$

$$r_5 = k_9 \theta^2_{H.S} - k_{10} P_{H_2} \theta^2_v$$

6. $C.S \xrightarrow{k_{11}} C_{Ni,F} + S$

   $C_{Ni,F} + S \xrightarrow{k_{12}} C.S \quad -r_{C.S} = r_{C_{Ni,F}}$

k_{11} and k_{12} are not converted to k'_{11} and k'_{12} because there is no need to multiply by C_{tot}/C_{tot}.

$C_{C.S} \Rightarrow \frac{mol}{gcat}$ $C_{Ni,F} \Rightarrow \frac{mol}{m^3 Ni}$ Units are different.

$$C_{Ni,F}\left(\frac{mol}{gcat}\right) = C_{Ni,F}\left(\frac{mol}{m^3 Ni}\right) \times \frac{1}{\rho_{Ni}}\left(\frac{m^3 Ni}{gNi}\right) \times Ni\%\left(\frac{gNi}{gcat}\right)$$

$$C_{Ni,F}\left(\frac{mol}{gcat}\right) = C_{Ni,F}\left(\frac{mol}{m^3 Ni}\right) \times \frac{1}{8.9 \times 10^6}\left(\frac{m^3 Ni}{gNi}\right) \times \frac{5}{105}\left(\frac{gNi}{gcat}\right)$$

$$C_{Ni,F}\left(\frac{mol}{gcat}\right) = C_{Ni,F}\left(\frac{mol}{m^3 Ni}\right) \times 5.35 \times 10^{-9}$$

$$\left[-\frac{dC_{C.S}(mol/gcat)}{dt}\right]_{R6} = \left[\frac{dC_{C_{Ni,F}}(mol/gcat)}{dt}\right]_{R6} = \left[\frac{d\left(C_{C_{Ni,F}}(mol/m^3 Ni) \times 5.35 \times 10^{-9}\right)}{dt}\right]_{R6}$$

$$\left[-\frac{dC_{C.S}}{dt}\right]_{R6} = k_{11}C_{C.S} - k_{12}C_{Ni,F}C_v$$

$$\left[-\frac{d(\theta_{C.S}C_{tot})}{dt}\right]_{R6} = k_{11}C_{C.S} - k_{12}C_{Ni,F}C_v$$

$$\left[-\frac{d\theta_{C.S}}{dt}\right]_{R6} = k_{11}\frac{C_{C.S}}{C_{tot}} - k_{12}C_{Ni,F}\frac{C_v}{C_{tot}}$$

$$\left[-\frac{d\theta_{C.S}}{dt}\right]_{R6} = k_{11}\theta_{C.S} - k_{12}C_{Ni,F}\theta_v$$

$$r_6 = k_{11}\theta_{C.S} - k_{12}C_{Ni,F}\theta_v$$

$$\left[\frac{d\left(C_{C_{Ni,F}}(mol/m^3 Ni) \times 5.35 \times 10^{-9}\right)}{dt}\right]_{R6} = k_{11}\theta_{C.S} - k_{12}C_{Ni,F}\theta_v = r_6$$

$$\left[\frac{dC_{C_{Ni,F}}(mol/m^3 Ni)}{dt}\right]_{R6} = \frac{k_{11}\theta_{C.S} - k_{12}C_{Ni,F}\theta_v}{5.35 \times 10^{-9}} = \frac{r_6}{5.35 \times 10^{-9}}$$

$$\left[\frac{dC_{C_{Ni,F}}(mol/m^3 Ni)}{dt}\right]_{R6} = \left[\frac{d(x_F(gC/gNi) \times 7.42 \times 10^5)}{dt}\right]_{R6} = \frac{k_{11}\theta_{C.S} - k_{12}C_{Ni,F}\theta_v}{5.35 \times 10^{-9}} = \frac{r_6}{5.35 \times 10^{-9}}$$

$$\rho_{Ni} = \frac{8.9 \times 10^6 gNi}{m^3 Ni}$$

$$C_{Ni,F}(molC/m^3) = x_F(\frac{gC}{gNi}) \times \frac{1}{MW_{carbon}}(\frac{1mol}{12gC}) \times \rho_{Ni}(\frac{8.9 \times 10^6 gNi}{m^3})$$

$$C_{Ni,F}(molC/m^3) = x_F(\frac{gC}{gNi}) \times 7.4197 \times 10^5$$

$$\left[\frac{dx_F(gC/gNi)}{dt}\right]_{R6} = \frac{k_{11}\theta_{C.S} - k_{12}C_{Ni,F}\theta_v}{(5.35\times10^{-9})(7.42\times10^5)} = \frac{r_6}{39.697\times10^{-4}}$$

As a result:

$$\boxed{\begin{array}{l}\left[-\frac{dC_{C.S}(mol/gcat)}{dt}\right]_{R6} = 5.35\times10^{-9}\left[\frac{dC_{C_{Ni,F}}(mol/m^3Ni)}{dt}\right]_{R6} \\ = 5.35\times10^{-9}\times7.42\times10^5\left[\frac{dx_F(gC/gNi)}{dt}\right]_{R6} = k_{11}\theta_{C.S} - k_{12}C_{Ni,F}\theta_v = r_6\end{array}}$$

A simple Langmuir equation can instead be used:

$$\frac{\theta_{C.S}}{1-\theta_{C.S}} = \frac{x_F}{1-x_F}\exp\left(-\frac{\Delta G_{seg}}{RT}\right)$$

where $\theta_{C.S}$ is the surface coverage of carbon, with ΔG_{seg} = -45,217 – 14.24 T (J/mol)

Therefore, the concentration of carbon in the nickel in the front, x_F (g carbon/g Ni) can be determined from the following equation:

So, $x_F = \frac{\theta_{C.S}}{[1-\exp(-\Delta G_{seg}/RT)]\theta_{C.S}+\exp(-\Delta G_{seg}/RT)}$

(Chen et al.[10]; Snoeck et al.[14])

7. $C_{Ni,F} \Rightarrow C_{Ni,R}$

Rate of diffusion of carbon through nickel particle was used to determine the specific weight of carbon in the model.

$$C_{Ni,F}\left(\frac{mol}{gcat}\right) = C_{Ni,F}\left(\frac{mol}{m^3Ni}\right)\times\frac{1}{\rho_{Ni}}\left(\frac{m^3Ni}{gNi}\right)\times Ni\%\left(\frac{gNi}{gcat}\right)$$

$$\left[\frac{dC_{C_{Ni,F}}(mol/m^3Ni)}{dt}\right]_{R7} = -\frac{D_{C_{Ni}}}{l}.(C_{C_{Ni,R}} - C_{C_{Ni,F}}).A_{Ni} = r_7$$

$$\left[\frac{dC_{C_{Ni,F}}(mol/m^3Ni)}{dt}\right]_{R7} = \left[\frac{C_{C_{Ni,F}}(mol/gcat)\times\rho_{Ni}(m^3Ni/gNi)/Ni\%(gNi/gcat)}{dt}\right]_{R7}$$
$$= -\frac{D_{C_{Ni}}}{l}.(C_{C_{Ni,R}} - C_{C_{Ni,F}}).A_{Ni}$$

$$\left[\frac{dC_{C_{Ni,F}}(mol/gcat)}{dt}\right]_{R7} = \frac{-\frac{D_{C_{Ni}}}{l}.(C_{C_{Ni,R}} - C_{C_{Ni,F}}).A_{Ni}}{8.9\times10^6\times\frac{105}{5}}$$

$$\left[\frac{dx_F(gC/gNi)}{dt}\right]_{R7} = \frac{-\frac{D_{C_{Ni}}}{l}.(C_{C_{Ni,R}} - C_{C_{Ni,F}}).A_{Ni}}{8.9\times10^6\times\frac{105}{5}\times\frac{1}{7.42\times10^5}}$$

$$\left(\frac{dx_F}{dt}\right)_{R7} = \frac{7.42\times10^5\times5}{8.9\times10^6\times105}\left(\frac{D_{C_{Ni}}}{l}.(7.42\times10^5x_F - C_{C_{Ni,R}}).A_{Ni}\right) = 0.0397\times r_7$$

r_7 = Rate of carbon diffusion through nickel (mol C/g_{cat} h)

$l =$ The average path length, which is assumed as 2/3 of nickel diameter

$= (2/3)\ \mathrm{d}_{Ni} = (2/3) \times 112\ \mathrm{nm} = (2/3) \times 112 \times 10^{-9}\ \mathrm{m} = 74.67 \times 10^{-9}\ \mathrm{m}$

$D_{C_{Ni}} =$ Diffusivity of carbon in nickel

$= 4.0 \times 10^{-9}\ \mathrm{cm}^2/\mathrm{s} = 1.44 \times 10^{-9}\ \mathrm{m}^2/\mathrm{h} = 2.4 \times 10^{-11}\mathrm{m}^2/\mathrm{min}$

$C_{C_{Ni,F}} =$The concentration of carbon dissolved in nickel at the front of Ni (mol C/m^3)

$C_{C_{Ni,R}} =$ The concentration of carbon dissolved in nickel at the rear of Ni (mol C/m^3)

$\mathrm{A}_{Ni} =$ Specific surface area of nickel particle

$= 0.15\ \mathrm{m}^2/\ \mathrm{g}_{cat}$

(Chen et al.[10])

8. $C_{Ni,R} \Leftrightarrow C_f$

This reaction is too fast; that is why it can be assumed that every mole of carbon that reaches the rear of Ni particle immediately contributes to the structure of the filament. So $C_{Ni,R}$ can be neglected in the model.

9. $nC.S \Rightarrow nC_p \quad -r_{C.S} = r_{C_p}$

The rate constant of the encapsulation reaction is the unknown parameter that is estimated throughout the model.

$$\left[-\frac{dC_{C.S}}{dt}\right]_{R9} = k'_{13}C^n_{C.S} \quad \left[-\frac{d(\theta_{C.S}C_{tot})}{dt}\right]_{R9} = k'_{13}C^n_{C.S} \quad \left[-\frac{d\theta_{C.S}}{dt}\right]_{R9} = C^{n-1}_{tot}k'_{13}\frac{C^n_{C.S}}{C^n_{tot}}$$

$$\left[-\frac{d\theta_{C.S}}{dt}\right]_{R9} = \underbrace{C^{n-1}_{tot}k'_{13}}_{k_{13}}\theta^n_{C.S} \quad \left[-\frac{d\theta_{C.S}}{dt}\right]_{R9} = k_{13}\theta^n_{C.S} \quad r_9 = k_{13}\theta^n_{C.S}$$